Available online at www.sciencedirect.com

ScienceDirect

Ceramics International 40 (2014) 2461–2466

CERAMICS INTERNATIONAL

www.elsevier.com/locate/ceramint

A gradient LMAS interlayer joint of SiC coated C/C composites to LAS glass ceramics

Fu Qian-Gang*, Peng Han, Li He-Jun, Wang Jie, Zhu Qing

C/C Composites Research Center, Science and Technology on Thermalstructural Materials Laboratory, Northwestern Polytechnical University, Xi'an 710072, PR China

Received 17 June 2013; received in revised form 28 July 2013; accepted 5 August 2013
Available online 9 August 2013

Abstract

A gradient Li_2O–MgO–Al_2O_3–SiO_2 (LMAS) glass ceramics interlayer was designed and prepared by vacuum hot-pressing to join SiC coated carbon/carbon (C/C) composites and Li_2O–Al_2O_3–SiO_2 (LAS) glass ceramics. The SiC transition layer could effectively infiltrate into the C/C substrates and firmly adhere to the LMAS interlayer. Both the Mg content and microhardness decreased gradually from the SiC side to the LAS glass ceramics side in the gradient LMAS interlayer. The thermal expansion coefficient (CTE) of LMAS glass ceramics increased with the increase of Mg content. The obtained shear strength of the welded sample with a gradient interlayer design was about 30.7% higher than that of the sample without the gradient design. The gradient LMAS interlayer could effectively improve the distribution of process-induced thermal stress in the joint, relieve the mismatch of CTE between SiC transition layer and LAS glass ceramics and increase the bonding strength of the joint.

Keywords: A. Joining; D. Glass ceramics; Gradient interlayer

1. Introduction

Glass ceramics possess wide ranging outstanding properties and have been used in spaceflight, chemistry, mechanism, and electromagnetism fields [1]. The Li_2O–Al_2O_3–SiO_2 (LAS) glass ceramics, with low-expansion, high electrical resistivity and chemical durability, are known for their application in heat-resistant windows and telescope mirror blanks [2]. However, the intrinsic brittleness of LAS glass ceramics limits their application. Although introducing suitable fibers and particles could improve the toughness of ceramics [3], new phases might affect the properties of LAS glass ceramics [4,5]. Carbon/carbon (C/C) composites have favorable high temperature mechanical properties and low density, which have been widely used in aerospace field [6]. Joining of these two materials is a possible way to benefit from the functional features given by LAS glass ceramics as well as the favorable mechanical properties given by C/C composites.

Unfortunately, LAS glass ceramics have poor wettability on C/C composites [7]. Thus, SiC was introduced as a modified layer [8]. However, the shear strength of SiC modified C/C–LAS joint was only 10 MPa without a joining layer, and it fractured at the SiC/LAS interface since the poor wettability and mismatch of thermal expansion coefficients (CTE) between SiC transition layer and LAS glass ceramics [9,10]. It is known that MgO–Al_2O_3–SiO_2 (MAS) glass ceramics have good wettability to SiC ceramic [11], low CTE and good mechanical properties up to 1000 °C [12]. To release the stress between SiC coating and LAS glass ceramics, a multilayer structure interlayer consisting of MAS and LAS was introduced and the shear strength was 17.9 MPa [13].

Given that the gradient distribution of element could further release the residual stress resulting from the CTE mismatch between different materials [14,15], a gradient Li_2O–MgO–Al_2O_3–SiO_2 (LMAS) glass ceramics joining layer was designed to improve the shear strength of the C/C–LAS joints

*Corresponding author. Tel.: +86 29 88494197; fax: +86 29 88495764.
E-mail address: fuqiangang@nwpu.edu.cn (Q.-G. Fu).

0272-8842/$ - see front matter
http://dx.doi.org/10.1016/j.ceramint.2013.08.021

in the present work. The microstructure, element distribution and mechanical properties of C/C–LAS joints with gradient joining layer were investigated.

2. Experimental

2.1. The preparation of C/C composites and glass powders

The C/C composites were consisted of polyacrylonitrile (PAN) derived carbon fibers in a pyrocarbon matrix. The carbon fiber preform was composed of 0°/90° continuous PAN carbon fibers and sandwiched with short PAN carbon fiber felts by needling. The carbon matrix was fabricated by a chemical vapor infiltration technique using natural gas as precursor. Finally, the density of C/C composites reached about 1.75 g/cm^3, and the overall fiber volume fraction of the material is about 25%. The interlaminar and in-plan shear strength (tested according to ASTM C1292 [16]) of C/C composites were 15 MPa and 32 MPa respectively [17]. After being polished, the specimens ($20 \times 30 \times 3$ mm^3) were ultrasonically cleaned by alcohol, and dried at 80 °C.

To prepare the MAS glass powders, 10–25 wt% MgO, 10–25 wt% Al_2O_3 and 40–55 wt% SiO_2 were thoroughly mixed. Subsequently, the mixture was melted in a corundum crucible at 1550–1600 °C for 2 h, and then quenched to room temperature in water. Finally, the glass was crushed and ground into powders with the size of 300 meshes.

LAS glass powders, used for sintering of LAS glass ceramics and preparing gradient interlayer, were made in the same way. The only difference was that the composition of raw powders was 10–15 wt% Li_2CO_3, 10–25 wt% Al_2O_3, and 60–80 wt% SiO_2. The softening point of the as-obtained MAS and LAS glass were 800 °C and 992 °C respectively, which were reported in our previous work [9].

The powders for preparing the SiC layer by pack-cementation method were composed of 50–75 wt% Si, 5–10 wt% graphite and 15–25 wt% Al_2O_3. Details for preparing the SiC interlayer were reported in Ref. [18]. After preparation of SiC transition layer on the C/C composites, the specimens were ultrasonically cleaned by alcohol and dried at 80 °C for the next step.

2.2. The joining of C/C composites and LAS glass ceramics with gradient interlayer

The MAS glass powders were homogeneously dispersed in ethanol and deposited on the ultrasonically cleaned surface of SiC transition layer. Then the sample was dried at 80 °C to remove the ethanol. The mixture of 50 wt% LAS and 50 wt% MAS glass powders were dispersed in ethanol to make the second slurry, which was applied on the first slurry in the same way. Thus, the preparation of gradient joining layer was accomplished. Then, the specimen was put into a graphite clamp, and dry LAS glass powders were evenly spread on the surface of gradient joining layer followed by a vacuum hot-pressing procedures at 1200–1300 °C for 10–40 min with the pressure of 20–25 MPa. Schematic of the gradient C/C–LAS joint is showed in Fig. 1. A group of comparative samples without a gradient joining layer design, i.e. the joining layer was a single MAS glass layer, which was also prepared through the same process.

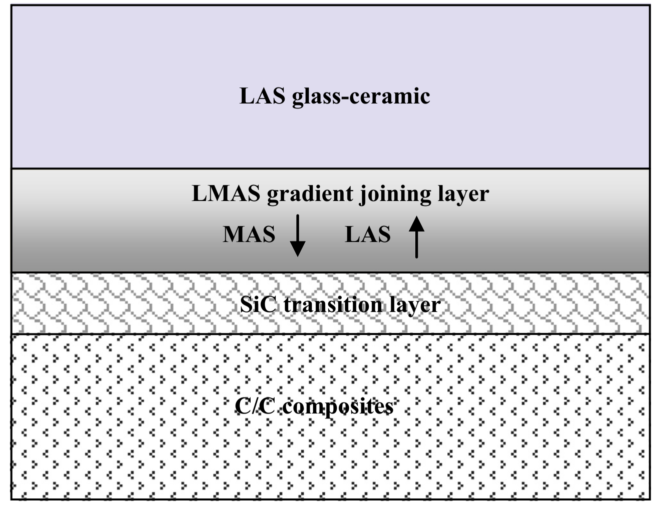

Fig. 1. Schematic of the gradient C/C–LAS joint.

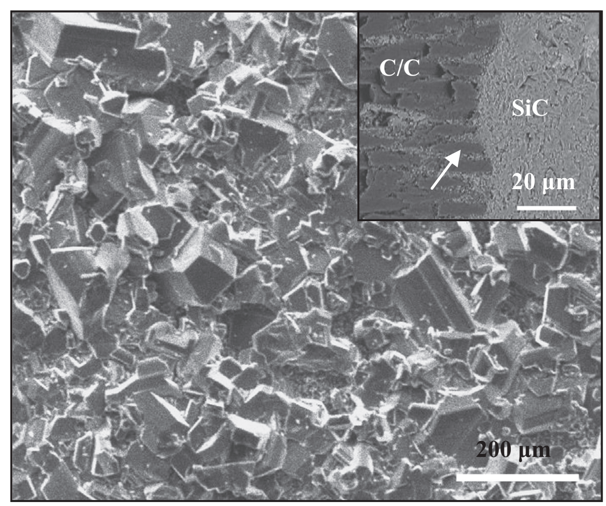

Fig. 2. SEM surface image of the SiC transition layer on C/C sample (inset refers to the cross section of the SiC transition layer on C/C sample).

2.3. Characterization

As for the shear strength tests, single-lap compressive shear test was chosen since it was easy to conduct rapidly and the amount of material required per test specimen was minimal [19]. It is worth to note that the stress distribution in the middle of the joint also combines a shear stress and a traction normal stress, and that the results are not appropriate for the safety designing of engineering components [20]. The joined specimen with the size of $10 \times 8 \times 6$ mm^3 was fixed in a device and compressed using a CMT5304-30KN universal test machine with a loading rate of 0.5 mm/min. The shear direction was parallel to the stacking direction of the carbon felt to avoid the failure of C/C composites.

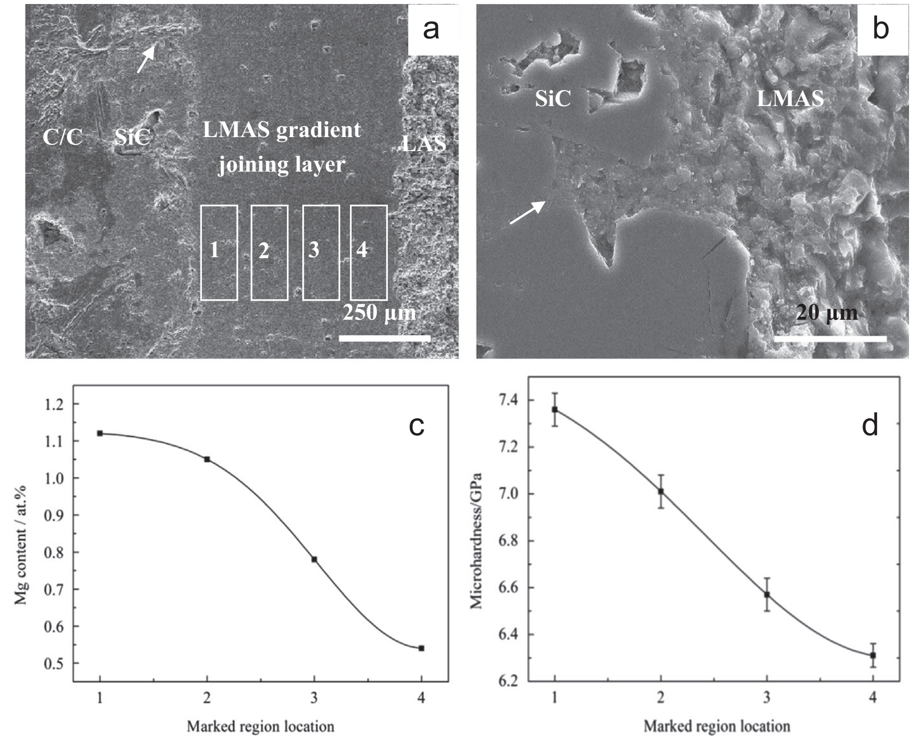

Fig. 3. Microstructure of C/C–LAS gradient joint, element distributions and microhardness of interlayer: (a) cross section image of gradient C/C–LAS joint; (b) enlarged view of SiC/LMAS interface; (c) Mg content and (d) microhardness of different regions marked in (a).

To measure the linear thermal expansion coefficient of the LMAS glass ceramics with different element content, mixtures of LAS and MAS glass powders with different proportions were hot-pressed using the same parameters for the joining process. Measurements of linear thermal expansion coefficients of LMAS glass ceramics were carried out on a thermal dilatometric analyzer (NETZSCH DIL 402 C) using an alumina bar as a standard. Specimen rods of about 13–15 mm length were measured from 30 °C up to 800 °C at a rate of 5 °C/min in Ar atmosphere. The linear thermal expansion coefficient was automatically calculated using the general equation:

$$\alpha = (\Delta L/L)(1/\Delta T) \quad (1)$$

where ΔL is the change in the original length (L) of the rod, ΔT is the temperature interval over which the samples were heated.

Microhardness measurement was carried out across the gradient interlayer with a Vickers microindenter on a MHT-M hardness tester under a load of 1 N and loading time of 15 s. The values are the average of at least 10 indents made on the different locations of the same area.

The microstructure, element distribution and fracture surface of C/C–LAS joints were analyzed by a VEGA TS5136XM scanning electron microscope (SEM) equipped with INCA-300 energy dispersive X-ray spectrometer (EDS).

The crystalline structure of the interlayer was measured with X-ray diffraction (XRD). The crystallinity degree of interlayer glass was determined by XRD method and calculated with the software Jade 6.0.

3. Results and discussion

3.1. Microstructure and morphological analysis

Fig. 2 shows the SEM micrograph on the surface of SiC transition layer, which displays a dense and uneven morphology. The SiC transition layer is composed of many large polygonal SiC grains and additional continuous phases. Inset of Fig. 3 refers to the cross section of the SiC transition layer on C/C samples. No obvious microcrack or defect can be observed in the interfacial region of SiC layer and C/C substrates, which gives evidence of good adhesion between SiC layer and C/C substrates. Besides, SiC has infiltrated into the C/C substrates through open pores and cracks formed during C/C fabrication process. Such infiltrated structure is beneficial, as the C/C–SiC interface was pinned tightly by the "micronails" (marked by white arrow).

Fig. 3a shows the cross section microstructure of C/C–LAS joint. Approximately 150 μm thick SiC layer and 500–600 μm thick gradient LMAS joining interlayer are observed between C/C composites and polyporous LAS glass ceramics. Some microcracks (marked by white arrow), caused by the mismatch of CTE between SiC and C/C composites, can be found in SiC transition layer. The gradient joining layer is relatively compact and homogeneous. However, some microholes still exit in this interlayer, since the gas did not fully discharge out of the glass powders during the hot pressing process. The cracks in SiC had no effect on the joining layer for the cracks did not propagate into this layer.

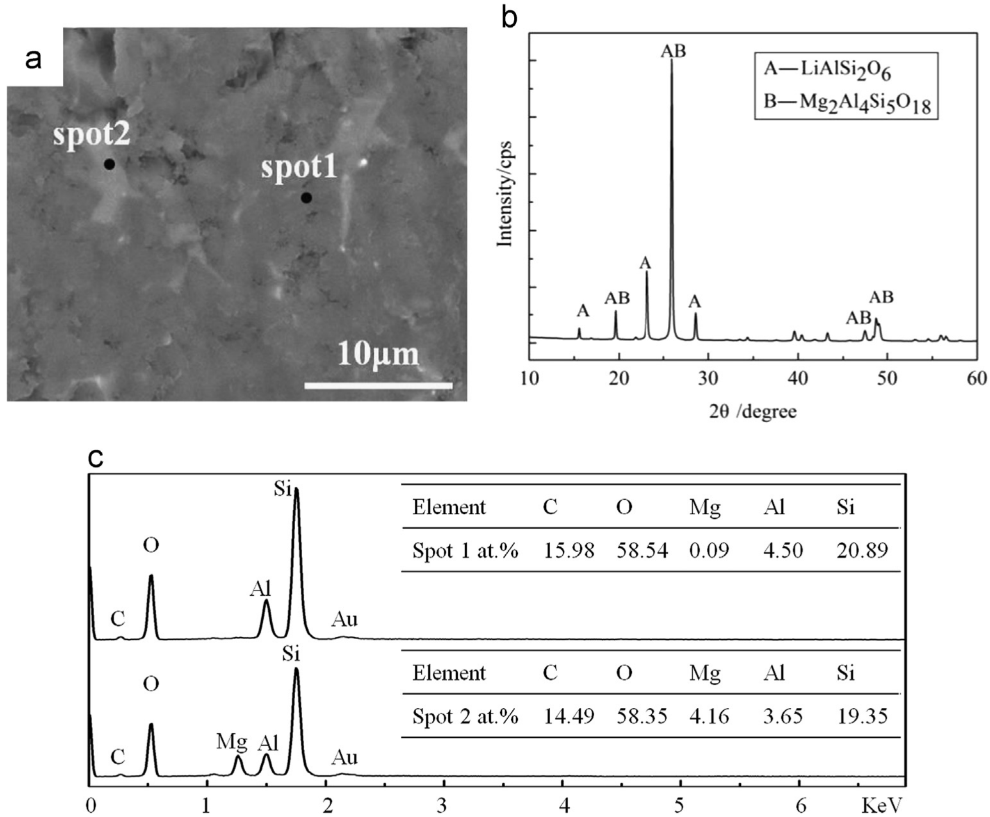

Fig. 4. BEI image, XRD pattern and EDS analysis of interlayer: (a) BEI image; (b) XRD pattern; and (c) EDS results of interlayer.

It can be observed that the gradient LMAS joining layer exhibits intimate contact with the SiC layer (Fig. 3b). At somewhere, LMAS can infiltrate into the SiC layer through the microholes on SiC surface, indicating that the LMAS joining layer has favorable fluidity and wettability on the SiC transition layer. In addition, the rough SiC surface is beneficial for forming a mechanical interlocking with gradient joining layer.

Fig. 3c and d shows the Mg content distribution and microhardness at marked regions of Fig. 3a. It is clear that a gradient joining layer was formed between the SiC transition layer and the LAS glass ceramics substrate. From the SiC interlayer to the LAS glass ceramics, the content of Mg element has a slight decrease and the microhardness decreases from 7.36 GPa to 6.31 GPa. Conditions of gradient constituent in the joining layer have been achieved by a gradient joining layer design. Actually, the gradient joining layer is a mutual diffusion layer of MAS and LAS. During the hot pressing procedure, Li in LAS glass ceramics and the second joining layer diffused into the first joining layer. Meanwhile Mg also diffuses under a concentration gradient. Though LAS glass ceramics can also diffuse into MAS joining layer without a gradient design, the diffusion distance is limited. And the design can facilitate the forming of a gradient joining layer.

Backscattering electron images of joining layer (Fig. 4a) reveals that, in the as-prepared joining layer, there are two kinds of crystalline particles characterized as dark gray (spot 1) and light gray (spot 2). Combining both XRD (Fig. 4b) and EDS (Fig. 4c) analyses, dark gray and light gray crystalline particles can be distinguished as spodumene (Li_2O–Al_2O_3–$2SiO_2$) and cordierite ($2MgO$–$2Al_2O_3$–$5SiO_2$) respectively. The existence of carbon in EDS analysis is probably because of the diffusion of SiC [21]. In addition, the crystallinity of LMAS matrix is approximately 87%, which was calculated using software Jade 6.0.

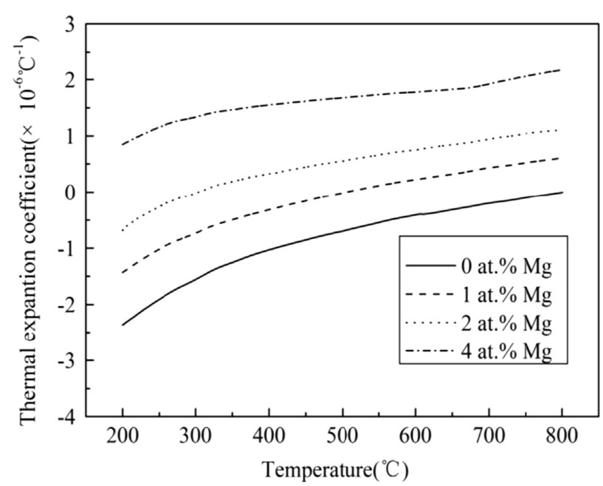

Fig. 5. Thermal expansion curves of LMAS glass ceramics with different Mg content.

Fig. 5 shows the CTE curves of the LMAS glass ceramics with varying content of Mg. It can be observed that the LAS glass ceramics have a negative CTE till to 800 °C.

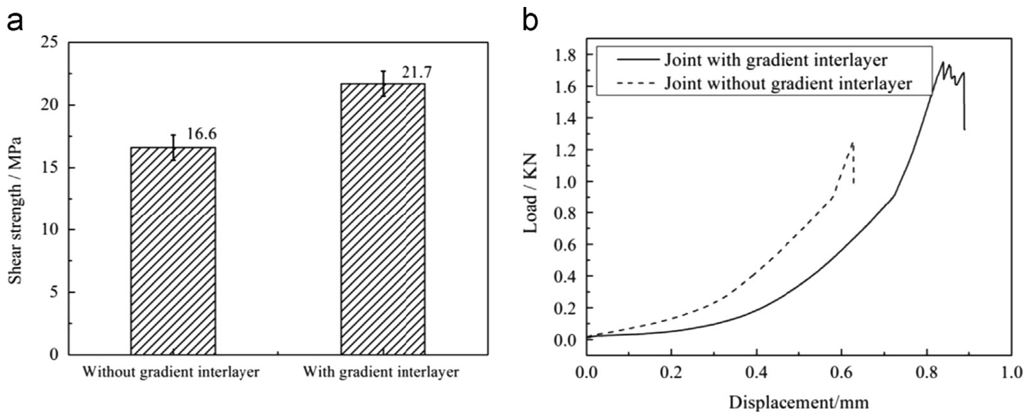

Fig. 6. Average shear strength of C–C/LAS joints without and with a gradient interlayer design.

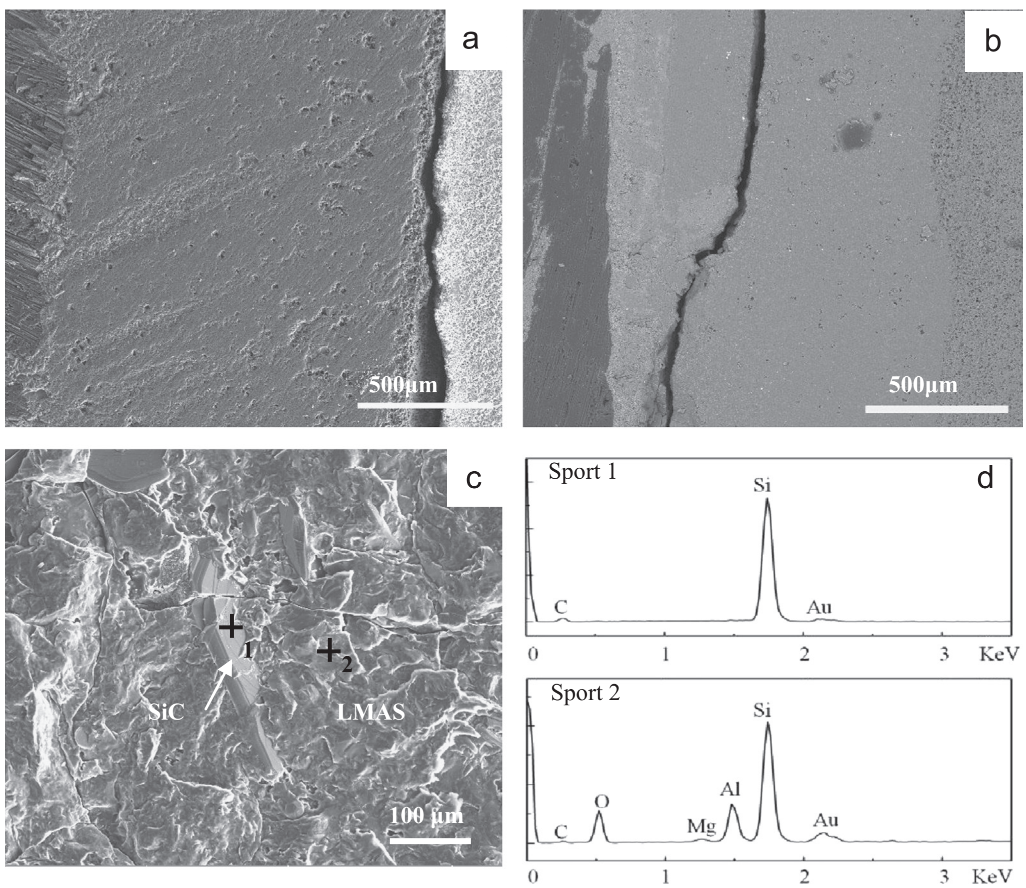

Fig. 7. Microstructures and EDS results of fractured samples after shear test: (a) cross section image without the gradient design; (b) with the gradient design; (c) fractured surfaces of gradient C/C–LAS joint; and (d) EDS results at two spots of fractured surface.

Additionally, the CTE of specimen bars increases with the increasing percent of Mg. When the content of Mg reaches 4 at %, the CTE of LMAS glass ceramics is $2.17\times10^{-6}\,^{\circ}C^{-1}$, which is much larger than that of LAS glass ceramics. Since the existence of thermal stress, the fracture occurs at the LMAS/LAS interface in the joint without the gradient interlayer. In the gradient C/C–LAS joints, the composition changes more gradually along the joining layer. The residual stress in the interface and internal joining layer is released due to the existence of composition gradient. Thus, the average shear strength of C/C–LAS joints with a gradient joining layer is largely increased.

3.2. Mechanical property

The average shear strength of C/C–LAS joints without the gradient joining layer design is 16.6 MPa, while that of the gradient joints is 21.7 MPa. It is 21% higher than that reported in Ref. [13]. Obviously, the design of gradient joining layer can help to promote the shear strength to a large extent. The load–displacement curves (Fig. 6b) show that the joint without gradient interlayer fractures suddenly when the load reaches its maximum. For the joint with gradient interlayer, non-destructive fractures happened several times before final fracture. It can be deduced that the propagation direction of main crack might change before ultimate failure.

As shown in Fig. 7a, the fracture occurs directly at the LMAS/LAS near interface of the joint without the gradient design. This kind of fracture type happens when there is a steep stress gradient at the interface [22]. While in the gradient joints, the cracks propagate through the SiC/gradient LMAS interface and then deflect into the internal gradient joining layer (Fig. 7b), which is consistent with the load–displacement curves. The crack deflection assumes more energy, which increases the shear strength to some extent. According to the fracture surface (Fig. 7c) and EDS analysis (Fig. 7d) of gradient C/C–LAS joints, a number of LMAS glass ceramics still adhere to SiC transition layer tightly. SiC grains can be observed in some areas, meaning that the fracture happens at the near interface of SiC transition layer and LMAS gradient joining layer. Big cracks penetrate through the SiC grains and LMAS glass ceramics, which is also beneficial to the improvement of shear strength for the consumption of plenty energy. The existence of the gradient interlayer relaxes the stress of LMAS/LAS interface effectively, and leads to the change of fracture model. That results in the increasing of energy dissipation and finally leads to the improvement of shear strength.

4. Conclusions

C/C composites have been successfully joined to LAS glass ceramics by vacuum hot-pressing technique using a SiC transition layer and a gradient LMAS joining layer. The interfaces were continuous and homogenous in C/C–LAS joints. The average shear strength of the joints with a gradient joining layer design is 21.7 MPa, which is 30.7% higher than that of the joints without a gradient design. The considerable improvement is attributed to the gradient joining layer, which plays an important role in releasing the thermal stress of the joints.

Acknowledgments

The authors of this work acknowledge funding supported from the National Natural Science Foundation of China (Grant nos. 51221001, 51222207 and 51272213), the “111” Program under Grant no. B08040, and Foundation for the Author of National Excellent Doctoral Dissertation of PR China 201036.

References

[1] X.Z. Guo, H. Yang, M. Cao, Nucleation and crystallization behavior of Li_2O–Al_2O_3–SiO_2 system glass ceramics containing little fluorine and no-fluorine, Journal of Non-Crystalline Solids 351 (2005) 2133–2137.

[2] O. García-Moreno, A. Fernández, R. Torrecillas, Conventional sintering of LAS–SiC nanocomposites with very low thermal expansion coefficient, Journal of the European Ceramic Society 30 (2010) 3219–3225.

[3] N.P. Bansal, CVD SiC fiber-reinforced barium aluminosilicate glass-ceramic matrix composites, Materials Science and Engineering: A 220 (1996) 129–139.

[4] F. Luo, H. Jiao, D.M. Zhu, W.C. Zhou, Dielectric properties of SiC/LAS composite, Materials Letters 59 (2005) 105–109.

[5] Z.B. Huang, W.B. Kang, Y.B. Qing, F. Luo, W.C. Zhou, D.M. Zhu, Influences of SiC_f content and length on the strength, toughness and dielectric properties of SiC_f/LAS glass-ceramic composites, Ceramics International 39 (2013) 3135–3140.

[6] E.L. Corral, L.S. Walker, Improved ablation resistance of C–C composites using zirconium diboride and boron carbide, Journal of the European Ceramic Society 30 (2010) 2357–2364.

[7] K.Z. Li, J. Wang, X.B. Ren, H.J. Li, W. Li, Z.Q. Li, The preparation and mechanical properties of carbon–carbon/lithium–aluminum–silicate composite joints, Materials and Design 44 (2013) 346–353.

[8] H.X. Zhu, K.Z. Li, J.H. Lu, H.J. Li, The effect of SiC coating on the joint of C/C and LAS, Key Engineering Materials 537 (2013) 24–27.

[9] X.B. Ren, H.J. Li, J.H. Li, L.J. Guo, J. Wang, X.R. Song, Influence of interlayer's thickness on strength of joints between LAS glass-ceramic and carbon/carbon composites, Journal of Inorganic Materials 8 (2011) 847–851.

[10] E. Bischoff, M. Ruhle, O. Sbaizero, A.G. Evans, Microstructural studies of the interfacial zone of a SiC-fiber-reinforced lithium aluminum silicate glass-ceramic, Journal of the American Ceramic Society 72 (1989) 741–745.

[11] H.L. Lee, S.W. Nam, B.S. Hahn, B.H. Park, D. Han, Joining of silicon carbide using MgO–Al_2O_3–SiO_2 filler, Journal of Materials Science 33 (1998) 5007–5014.

[12] F. Doreau, H. Maupas, D. Kervadec, P. Ruterana, J. Vicens, J.L. Chermant, The complexity of the matrix micro structure in SiC-fiber-reinforced glass ceramic composites, Journal of the European Ceramic Society 15 (1995) 1235–1247.

[13] H. Peng, Q.G. Fu, B.L. Jia, H.J. Li, Thermal shock resistance of SiC/MAS–LAS multilayer joint of carbon/carbon composites to LAS glass-ceramic, Materials Science and Engineering: A 556 (2012) 607–611.

[14] C.S. Lee, X.F. Zhang, G. Thomas, Novel joining of dissimilar ceramics in the Si_3N_4–Al_2O_3 system using polytypoid functional gradients, Acta Materialia 49 (2001) 3775–3780.

[15] J.X. Deng, L.L. Liu, M.W. Ding, Gradient structures in ceramic nozzles for improved erosion wear resistance, Ceramics International 33 (2007) 1255–1261.

[16] ASTM C1292-00 Standard Test Method for Shear Strength of Continuous Fiber-Reinforced Advanced Ceramics at Ambient Temperatures, 2005.

[17] K.F. Yan, Characterization and Distribution of Shear Strength for C/C and C/SiC, Master Degree Dissertation of Northwestern Polytechnical University, China, 2011.

[18] J.F. Huang, B. Wang, H.J. Li, M. Liu, L.Y. Cao, C.Y. Yao, A $MoSi_2$/SiC oxidation protective coating for carbon/carbon composites, Surface and Coatings Technology 201 (2007) 9444–9447.

[19] F. Rosselli, M.H. Santare, Comparison of the short beam shear (SBS) and interlaminar shear device (ISD) tests, Composites Part A 28A (1997) 587–594.

[20] M. Ferraris, A. Ventrella, M. Salvo, M. Avalle, F. Pavia, E. Martin, Comparison of shear strength tests on AV119 epoxy-joined carbon/carbon composites, Composites Part B 41 (2010) 182–191.

[21] A.L. Yurkov, B.I. Polyak, Contact phenomena and interactions in the system SiC–SiO_2–R_xO_y in condensed matter. Part II interactions between silicon carbide and silicate glasses at elevated temperatures, Journal of Materials Science 31 (1996) 2729–2733.

[22] P.X. Ai, Y.S. Zhou, Interlayer design for joining pressureless sintered sialon ceramic and 40Cr steel brazing with $Ag_{57}Cu_{38}Ti_5$ filler metal, Journal of Materials Science 27 (1992) 1560–1566.